Swiss J Geosci (2017) 110:547–563
DOI 10.1007/s00015-017-0269-0

Multi-scale imaging of a slow active fault zone: contribution for improved seismic hazard assessment in the Swiss Alpine foreland

Naomi Vouillamoz[1,3] · **Jon Mosar**[1] · **Nicholas Deichmann**[2]

Received: 3 October 2016 / Accepted: 16 March 2017 / Published online: 3 April 2017

Abstract Seismic hazard assessment of slow active fault zones is challenging as usually only a few decades of sparse instrumental seismic monitoring is available to characterize seismic activity. Tectonic features linked to the observed seismicity can be mapped by seismic imaging techniques and/or geomorphological and structural evidences. In this study, we investigate a seismic lineament located in the Swiss Alpine foreland, which was discussed in previous work as being related to crustal structures carrying in size the potential of a magnitude **M** 6 earthquake. New, low-magnitude ($-2.0 \leq M_L \leq 2.5$) earthquake data are used to image the spatial and temporal distribution of seismogenic features in the target area. Quantitative and qualitative analyses are applied to the waveform dataset to better constrain earthquakes distribution and source processes. Potential tectonic features responsible for the observed seismicity are modelled based on new reinterpretations of oil industry seismic profiles and recent field data in the study area. The earthquake and tectonic datasets are then integrated in a 3D model. Spatially, the seismicity correlates over 10–15 km with a N–S oriented sub-vertical fault zone imaged in seismic profiles in the Mesozoic cover units above a major decollement on top of the mechanically more rigid basement and seen in outcrops of Tertiary series east of the city of Fribourg. Observed earthquakes cluster at shallow depth (<4 km) in the sedimentary cover. Given the spatial extend of the observed seismicity, we infer the potential of a moderate size earthquake to be generated on the lineament. However, since the existence of along strike structures in the basement cannot be excluded, a maximum **M** 6 earthquake cannot be ruled out. Thus, the Fribourg Lineament constitutes a non-negligible source of seismic hazard in the Swiss Alpine foreland.

Keywords Microseismicity · Earthquake clustering · Neotectonics · Seismic imaging · GIS

1 Introduction

1.1 Overview

The Swiss Alpine foreland is an area of overall low seismic activity (e.g. Wiemer et al. 2009; Singer et al. 2014; Diehl et al. 2015). However, digital seismic data collected by the Swiss National Network since the late 1970's show a concentration of earthquakes that delineate a 20–30 km long N–S striking seismic lineament east of the city of Fribourg called the Fribourg Lineament (FL) (Fig. 1) (ECOS: Earthquake Catalog of Switzerland; Fäh et al. 2003, 2011). In the late 1980's and 1990's, three sequences of earthquakes including four events with local magnitudes M_L between 3 and 4 and one with M_L 4.3 occurred on the southern segment of the FL (Kastrup et al. 2004, 2007). Although the hypocentral depth of these events could be constrained at shallow depth (~2 km) using synthetic seismograms (Kastrup et al. 2007), a link with deep-seated faults, cutting the Mesozoic and Tertiary cover series, and rooting in the underlying basement was hypothesized. The

Editorial handling: C. Sue and S. Schmid.

✉ Naomi Vouillamoz
naomi.vouillamoz@geophys.uni-stuttgart.de

[1] Department of Geosciences, University of Fribourg, Chemin du Musée 6, 1700 Fribourg, Switzerland

[2] Swiss Seismological Service (SED), ETHZ, Sonneggstrasse 5, 8092 Zurich, Switzerland

[3] Present Address: Institute for Geophysics, University of Stuttgart, Azenbergstrasse 16, 70174 Stuttgart, Germany

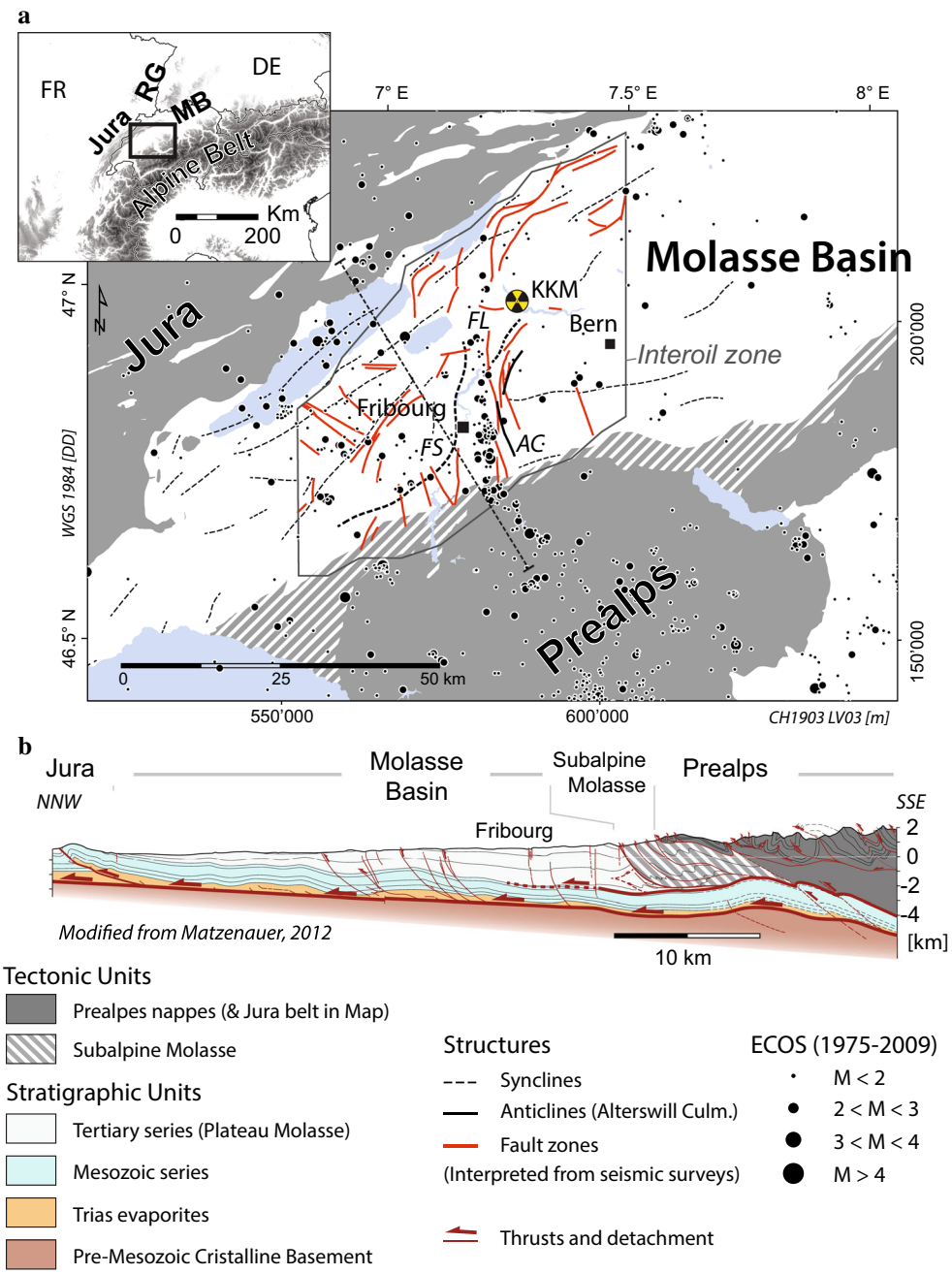

Fig. 1 **a** *Upper frame* location of the study area in the western Swiss Molasse basin (MB), south of the Rhine graben (RG). *General frame* simplified tectonic map. The Interoil zone encircles the region for which interpreted oil industry seismic profiles by (Interoil 2010) are available for this study and in which fault zones interpolated over the base Tertiary horizon are displayed. *Dotted lines* indicate main synclines; note the marked deviation of the Fribourg Syncline (FS) and the Alterswill culmination (AC-*bold lines*). The instrumental ECOS (1975–2009) (Fäh et al. 2011) features a prominent NS cluster of earthquakes east of the city Fribourg that ends close to the Mühleberg Nuclear Power Plant (KKM). **c** NNW–SSE structural cross-section through the western Swiss Molasse basin (Modified from (Matzenauer 2012), profile trace is shown in **b**). The western Swiss Molasse basin is interpreted as a top-wedge basin (Willett and Schlunegger 2010), where the sedimentary cover is passively transported and deformed on top of a basal detachment in the Triassic evaporites

N–S orientation of the tectonic structures in the Fribourg area was thus linked to crustal structures possibly representing a southward extension of the Rhine graben faults in the North (Nagra 1988; Berger and Gundlach 1990; Kastrup et al. 2007) (Fig. 1). As a consequence, the fault system was postulated to carry in size the potential of a moment magnitude **M** 6 earthquake (Kastrup et al. 2007).

The implications of this recent seismic activity have raised questions about the vulnerability of critical infrastructures such as the Mühleberg Nuclear Power Plant (KKM, Kernkraftwerk Mühleberg) located NE of Fribourg, as well as the city of Fribourg itself (Fig. 1). In a region of low seismicity, the only way to obtain additional information about the ongoing seismic activity and its tectonic context is to lower the detection threshold. Thus in this work, we propose to characterize the FL using low-magnitude earthquake data ($-2.0 < M_L < 2.5$) acquired in the period 2009–2013 by two new stations of the Swiss national network and two temporary seismic mini-arrays deployed in the Fribourg area (Vouillamoz et al. 2016). In particular, the thus substantially enlarged earthquake database is searched for evidence of seismic activity in the basement, in addition to the seismicity in the sedimentary

cover known from previous studies. Newly reinterpreted seismic imaging surveys (Interoil 2010; Meier 2010) are integrated with recent structural data (Ibele 2011) and geological information gathered from the literature (Vouillamoz 2015) and implemented in a GIS database from which a 3D fault model is constructed. The level of coincidence between the new earthquake data and the 3D fault model is used to discuss the possible link between interpreted fault zones and observed seismicity and to evaluate possible fault rupture scenarios with corresponding range of **M** max.

1.2 Tectonic setting

The area of investigation around the city of Fribourg is located in the western Swiss Molasse basin, between the thrusted Subalpine Molasse and the allochthonous Prealps *klippen* to the South and the Jura fold-and-thrust belt to the North (Fig. 1a, b). The Swiss Molasse basin initiated as a flexural foreland basin in response to the bending of the European lithosphere due to the southward subduction of the European lower plate under the colliding Adriatic plate in early Tertiary time (e.g. Singer et al. 2014; Schlunegger and Kissling 2015). Sedimentation started in the lower Oligocene and continued through Miocene times with progressive onlap towards the North on top of the underlying Mesozoic sediments (Homewood et al. 1986). As a result, the thickness of the Molasse units varies from a few hundred meters in the North to more than 4 km in the South (Naef et al. 1985; Laubscher 1987; Burkhard 1990; Burkhard and Sommaruga 1998; Sommaruga et al. 2012). According to the distant-push hypothesis (*Fernshub*) of Buxtorf (1907) (Laubscher 1961, 1997), the foreland basin subsequently evolved into a wedge-top basin coincident with the development of the Jura fold-and-thrust belt to the north (Bonnet et al. 2007; Willett and Schlunegger 2010). The whole foreland sedimentary cover is thereby detached above the mechanical basement along a main decollement level in the Lower–Middle Triassic evaporites (Fig. 1b) in relation with exhumation and imbrication of the External Crystalline Massifs in the Alps (Sommaruga 1995; Burkhard and Sommaruga 1998; Sommaruga 1999). Whereas the Jura Mountains exhibit an important fault-and-thrust related folding, the structures in the Molasse basin remain of modest amplitude, inhibited by the increasing thickness of the Tertiary sediment cover towards the south (Schuppli 1950; Jordi 1951; Sommaruga et al. 2012).

At its southern edge, the Molasse basin is in contact with the imbricated Subalpine Molasse (Schuppli 1950; Jordi 1951). There, the Tertiary cover is decoupled from the underlying Mesozoic series, the latter in turn being decoupled and detached from the mechanical basement along the basal decollement. This north-directed major thrust zone correlates with the young and out of sequence thrusting of the Alps (Fig. 1b) (Cederbom et al. 2011; von Hagke et al. 2012). The general NE–SW oriented alpine trend of folds in the Molasse basin and Jura fold-and-thrust belt shows a deviation east of the city of Fribourg to form the Fribourg structure or Fribourg zone (Fig. 1). The Fribourg syncline turns into a N–S direction along strike of the topographic ridge of the Alterswill culmination (Plancherel 1996). This latter zone also bears an extended N–S trending fault zone arranged in an *en-échelon* array that is well imaged in seismic profiles in the Mesozoic units (Interoil 2010; Sommaruga et al. 2012). The area of investigation thus exhibits strain partitioning along two decollement levels (Base Mesozoic and Base Tertiary) (Bonnet et al. 2007) and regional vertical tear faults.

2 Earthquake data

2.1 Catalog design

The historical and instrumental seismicity of the Fribourg region up to the year 2004 is documented in Kastrup et al. (2007). This time period includes three prominent earthquake swarms in 1987, 1995 and 1999 with maximum magnitudes of M_L 3.9, 3.7 and 4.3, respectively. The earthquakes recorded routinely by the national broadband and strong-motion networks of the Swiss Seismological Service (SED) over the years 2005–2008, a period of relatively low seismic activity, are included in the ECOS catalog (Fäh et al. 2011).

Nanoseismic monitoring techniques (Wust-Bloch and Joswig 2006; Joswig 2008; Sick et al. 2014) were applied in the period 2009–2013 in order to lower the detection threshold compared to the seismicity recorded routinely by the SED in the Fribourg area (Vouillamoz et al. 2016). Low-magnitude earthquakes were detected by applying sonogram analysis (Sick et al. 2014) on continuous waveforms recorded at three stations operated by the SED (two new accelerometers SCOU, and STAF, and one broadband station TORNY), and two small aperture (<100 m) sparse seismic arrays (SNS) deployed temporarily close to the FL (Fig. 2). Data of six Swiss local broadband stations were further used to constrain the location of the stronger events (Fig. 2). A 1D layered velocity model, derived for the Fribourg region from the Swiss 3D velocity model (Husen et al. 2003) and refined in shallow layers based on deep borehole data (Abednego 2016), was used for event location (Vouillamoz et al. 2016).

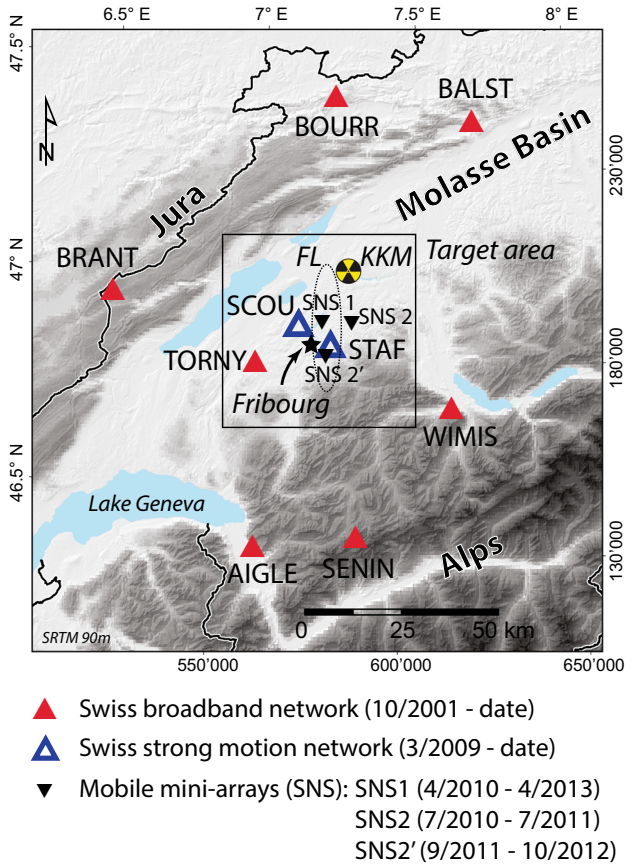

Fig. 2 Station network map and seismic records availability. The Swiss broadband and strong-motion networks are operated by the Swiss Seismological Service (SED). The Swiss permanent network was upgraded by two mobile seismic mini-arrays (SNS), operated by the University of Fribourg in the immediate vicinity of the FL between 2010 and 2013 (Vouillamoz et al. 2016)

2.2 The Fribourg earthquake catalog 2009–2013

Over the period 2009–2013, the Fribourg earthquake catalog (FRICAT) comprises 270 low-magnitude events ($-1.7 < M_L < 1.5$) and 34 events ($0.4 < M_L < 2.5$) detected also by the SED (ECOS events) that were recorded in the period 2009–2013 in a 2500 km^2 around the city of Fribourg. The 304 events were processed and merged into a joint uniform database using HypoLine software (Joswig 2008; Vouillamoz et al. 2016). The signal quality of half of the Fribourg events was sufficiently high to enable a reliable location, with epicentral uncertainty below 2 km. Because of poor SNR (signal to noise ratio) of the onsets, the remaining 50% of the events are either located with lower confidence (up to 5 km of epicentral uncertainty, 20% of the dataset) or not locatable (30% of the dataset) (Vouillamoz et al. 2016). Although their location is problematic or undefined, these events are preserved in the database as their source origin is further constrained using waveform similarity analyses.

3 Characterizing Fribourg microseismicity using waveform data

3.1 Absolute hypocenter locations

The 50% of quality events feature two zones of apparent enhanced seismicity (Fig. 3a): (1) the FL, and (2) the Fribourg cluster, a region with earthquake clustering below the city of Fribourg. As detailed in Vouillamoz et al. (2016), for 129 quality events a hypocenter solution could be resolved: resulting focal depths range within 500 m and 4 km depth with a predominance in the Tertiary cover series at depth below 2 km (107 events, 83% of the events with resolved hypocenter solution) (Fig. 3b, c).

Based on synthetic-seismogram modeling of waveforms and travel-time differences of the downgoing P-wave reflected at the Moho (PMP) and the upgoing S-wave reflected and converted to a P-wave at the Earth's surface before being reflected at the Moho (sPMP), Kastrup et al. (2007) concluded that the hypocenters of the earthquake sequences of 1987, 1995 and 1999 along the FL were located within the sedimentary cover at a depth of only 2 km. A comparison of the seismograms of the two higher-magnitude ECOS events recorded in 2009 along the FL with the corresponding seismogram of one of the 1995 events shows that the sPMP-PMP travel-time differences are almost identical (see Fig. 10 of Deichmann et al. 2010) and that therefore their focal depths must be similar. Thus, the shallow focal depths shown in Fig. 3b, c agree with other independent focal depth estimates in Fribourg region.

3.2 Constraining relative epicenter distribution using station network geometry

We take advantage of the Swiss station network geometry to better constrain the relative epicenter distribution of events in Fribourg region. Twelve higher-magnitude events detected by the national network are selected for a qualitative waveform analysis (Fig. 4). On an E–W profile, the relative epicenter distribution of the 12 events is evaluated by looking at the signals recorded at HASLI, which lies due east of the FL (Fig. 4a). Due to substandard SNR of P-arrivals at HASLI (>70 km distant), the waveforms are aligned on unequivocal P-arrivals identified at TORNY, which lies due west of the FL. S-arrivals recorded at HASLI display a consistent alignment for events located on the FL, whereas S-arrivals of events related to the Fribourg cluster (event number 4–6) are delayed by a few seconds (Fig. 5a). The consistent alignment of S-arrivals recorded due east of the events (and aligned on phase arrivals recorded due west) corroborates previous results by Kastrup et al. (2007) showing that epicenters along the FL

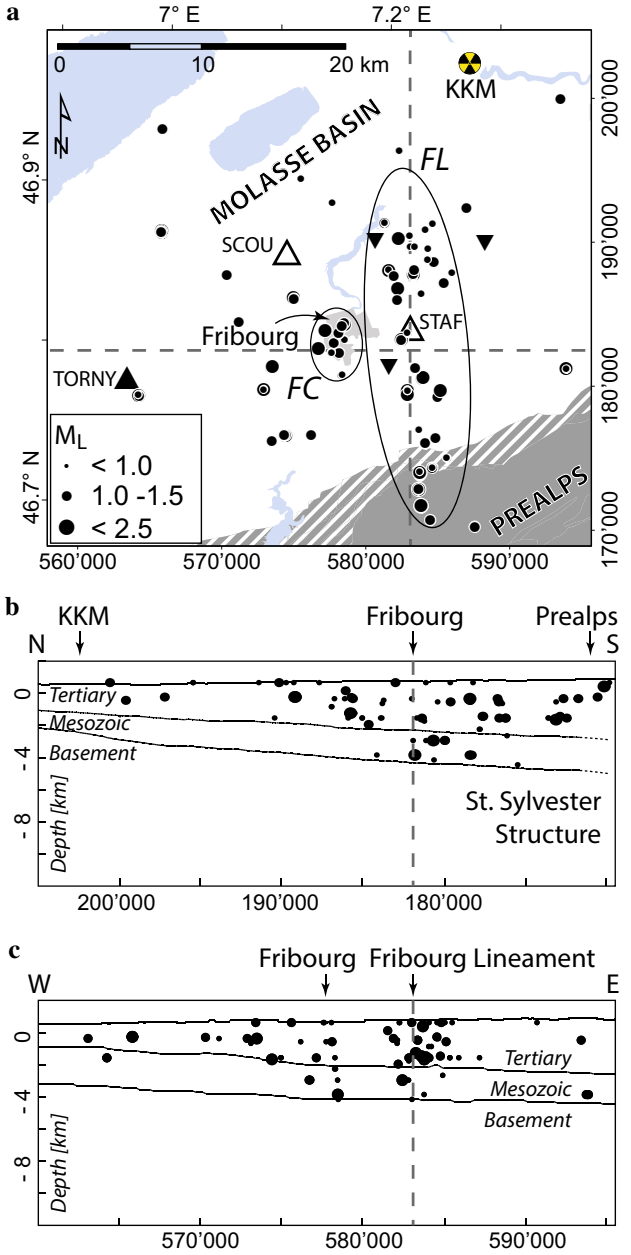

Fig. 3 **a** Fribourg high-quality events (epicentral uncertainty <2 km) highlight two zones of apparent clustered seismicity: the Fribourg Lineament (FL) and the Fribourg Cluster (FC) below the city of Fribourg. **b**, **c** N–S (E 583′000) and W–E (N 182′000) hypocenter projections. Base Tertiary and Base Mesozoic horizon are interpolated from seismic imaging surveys (Interoil 2010). Resolved focal depths are restricted to the sedimentary cover (Vouillamoz et al. 2016)

must be closely spaced in an E–W direction. The offset in S-arrivals between signals related to the FL and the Fribourg cluster is evidence for the existence of two distinct active tectonic features on an E–W profile in Fribourg area.

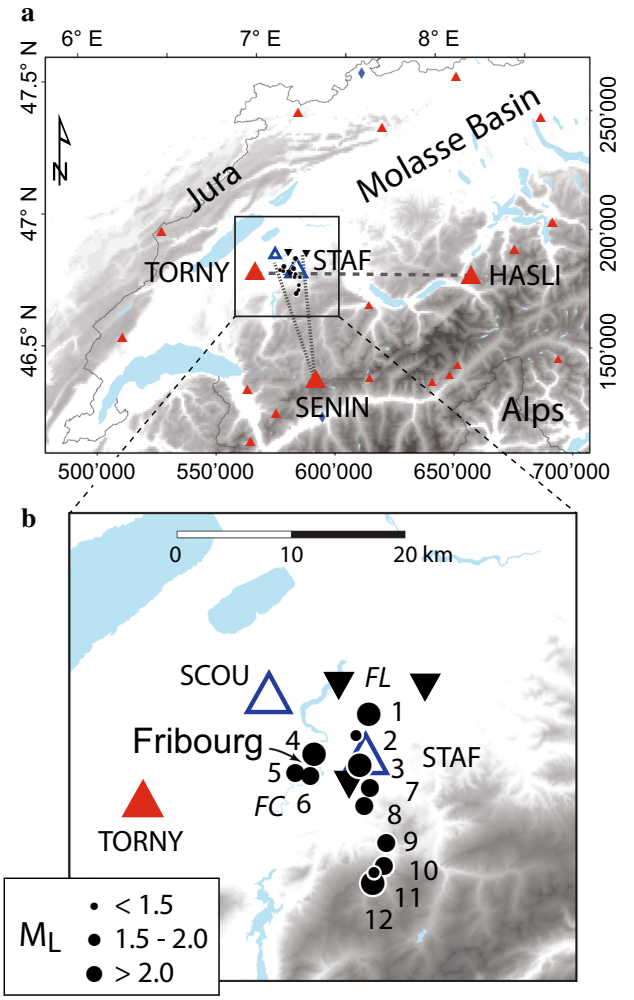

Fig. 4 **a** Station map and **b** zoom showing the location of twelve higher-magnitude ECOS events between 2009 and 2013 along the Fribourg Lineament (*FL*) and the Fribourg Cluster (*FC*) relative to the local station network

Increasing S–P travel-time differences from south (event number 12) to north (event number 1) on the signals recorded south of Fribourg at SENIN (Fig. 4a) suggests a N–S distribution of the selected events (Fig. 5b). The waveforms recorded at STAF, which lies on the FL (Fig. 4a), display a systematic pattern of S-P travel-time differences as a function of their location from north to south along the FL and within the Fribourg cluster (Fig. 5c, d). The prominent surface waves observed on vertical traces at such short epicentral distances are additional evidence for a shallow hypocentral depth of the events (Deichmann et al. 2010). Thus, it can be concluded that the epicenters of the 12 selected events are distributed with a preferred N–S orientation along two seismogenic zones: the FL and the Fribourg cluster.

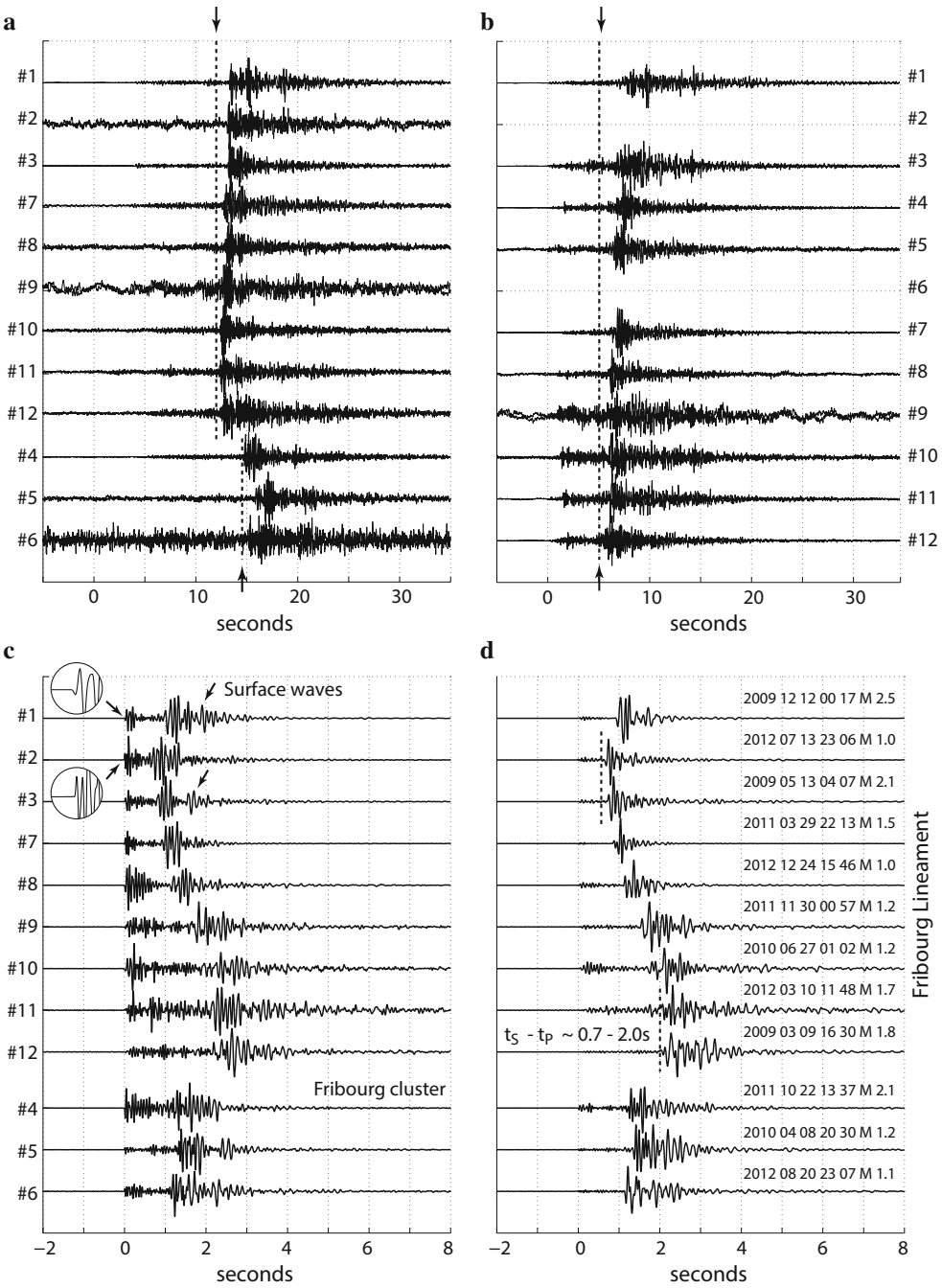

Fig. 5 Seismograms (nm/s, 2–10 Hz) of twelve higher-magnitude ECOS events (see location in Fig. 7b). **a** Signals recorded at HASLI aligned on unequivocal P-arrivals identified at station TORNY. **b** Seismograms recorded at SENIN aligned on P-arrivals manually picked at that station. P-onsets of events number 2 and 6 could not be picked satisfactorily and are consequently not displayed. For better display of S-arrivals, vertical and east-horizontal components are stacked in **a**, **b**. **c** Seismograms recorded at STAF vertical channel display prominent surface waves at short epicentral distances (*arrows*). Note the different onset polarities (*zoomed circles*) that suggest variation in focal mechanism (see Sect. 6). **d** Signal recorded at STAF east-horizontal component show systematical variations in t_S–t_P travel-time differences between about 0.7 and 2.0 s and high-amplitude S-phase arrivals. The *vertical dotted lines* in **a**, **b**, **d** help to visualize waveform alignments

3.3 Spatial and temporal patterns of microseismicity using waveform similarity

Closely spaced earthquake families in microseismic datasets can be discriminated using simple cross-correlation analyses (e.g. Deichmann and Garcia-Fernandez 1992; Augliera et al. 1995; Cattaneo et al. 1999; Massa et al. 2006; Barani et al. 2007; Kraft and Deichmann 2014). In order to characterize the spatial and temporal evolution of clustered microseismic activity in the Fribourg area, we use the waveform dataset recorded at STAF (the closest station on the FL, see Fig. 2). To optimize cross-correlation results, only waveforms with P-onset SNR above two are selected. The 227 selected signals are cross-correlated in the time-domain, using a five-second window that includes P- and S-phases codas (receiver-source distances <20 km). The waveforms are integrated to velocity and aligned on manually picked P-arrivals; a second order Butterworth bandpass filter of 1–30 Hz is applied. The peak of the normalized cross-correlation function computed for all possible pair of events is then plotted in cross-correlation matrixes using a correlation index threshold of 0.8 (Fig. 6).

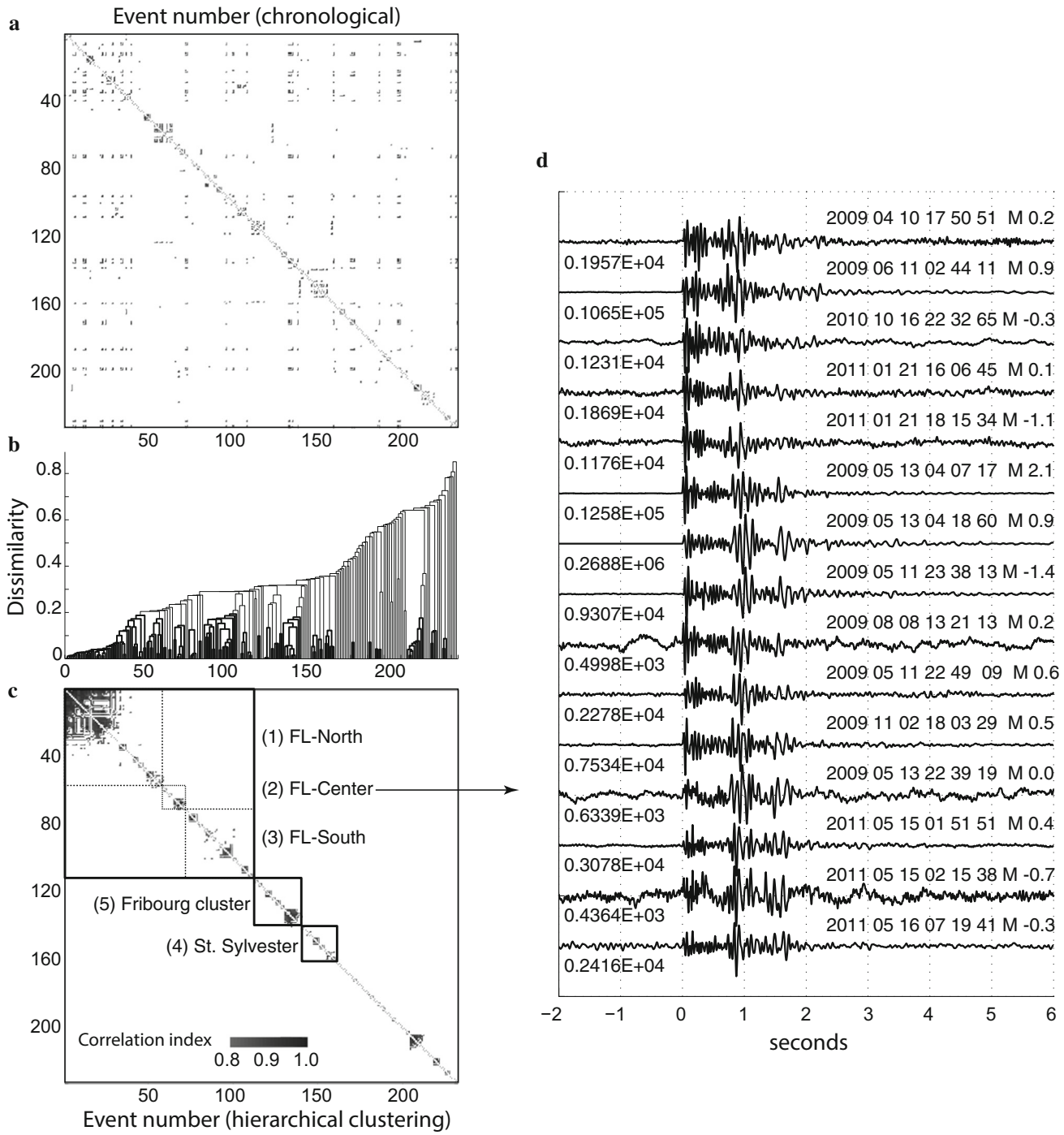

Fig. 6 **a** Cross-correlation matrix for 227 chronologically sorted events recorded at station STAF (five-second cross-correlation window aligned on P-arrivals, vertical component integrated to velocity and band-pass filtered between 1 and 30 Hz). **b** Hierarchical clustering derived with a single linkage function and a dissimilarity threshold of 0.2. **c** Cross-correlation matrix resulting from the hierarchical clustering. Five main earthquake families are highlighted in the Fribourg earthquake dataset in function of their relative location to STAF: (*1*) FL-North, (*2*) FL-Center, (*3*) FL-South, (*4*) St. Sylvester, and (*5*) Fribourg Cluster. (*d*) STAF vertical-component waveforms (nm/s, maximum 0-peak amplitude is indicated below each trace, 1–30 Hz) for the FL-Center cluster

A first matrix is derived using a chronological sorting of events (Fig. 6a). It displays numerous highly coherent pairs closely confined to the main diagonal. These on-diagonal pairs highlight frequent temporal clustering of events sharing a high waveform similarity, which in turn suggests spatial clustering of the corresponding events. The chronological matrix also displays off-diagonal pairs, signifying the existence of repeating seismic events in longer

time intervals (month–year). With the aim to identify earthquake families, a single linkage function (nearest neighbor, minimum method, Matlab^{TM}) is applied on the chronological cross-correlation dataset using a dissimilarity threshold of 0.2. The resulting dendrogram and cross-correlation matrix picture a few main earthquake families, gathering each several earthquake clusters (Fig. 6b, c). The epicenter distribution of the located events among each family is verified (Fig. 7) and shows that the agglomerated events distribute consistently in space. The clustered events are gathered into five main earthquake families following their location relative to STAF: (1) FL-North, (2) FL-Center, (3) FL-South, (4) St. Sylvester, and (5) Fribourg cluster (Figs. 6c, 7). A few other minor clusters correspond to sequences detected in the larger Fribourg area and are not considered here. The striking waveform similarity observed in individual clusters (Fig. 6d) suggests events tightly distributed in space that share common source mechanism (e.g. Deichmann and Garcia-Fernandez 1992; Augliera et al. 1995; Scarfì et al. 2003). Consequently, part of the scatter in epicenter locations within individual clusters or segments of the FL seen on the map in Fig. 7 is probably an artifact of the absolute location procedure. In fact, with the exception of the N–S extent of the St. Sylvester cluster, this scatter is well within the estimated epicenter location uncertainty of ±2 km for quality event. For the St. Sylvester cluster, the more important scatter is explained by a non-optimal station geometry, which results in large epicentral uncertainty in a N–S direction (see Fig. 7c of Vouillamoz et al. 2016).

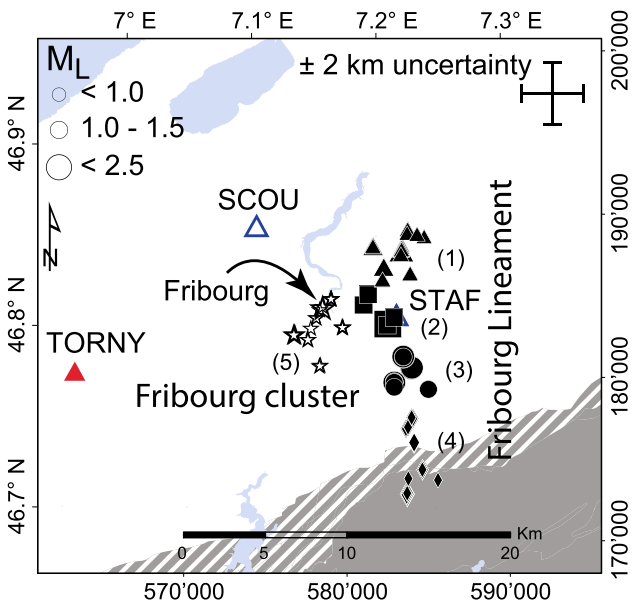

Fig. 7 Epicenter distribution of the located events in each of the five earthquake families derived by hierarchical clustering. *Triangles* (*1*) FL-North; *squares* (*2*) FL-Center; *circles* (3) FL-South; *diamonds*: (*4*) St. Sylvester; and *stars*: (*5*) Fribourg cluster

3.4 Temporal evolution of microseismic activity in Fribourg region

The local magnitude (M_L) of Fribourg events was calculated using a distance-attenuation function calibrated for weak shocks recorded at short epicentral distances (Wust-Bloch and Joswig 2006; Vouillamoz et al. 2016). For the sake of consistency, the M_L values are assigned also to those events after 2008 that were recorded by the SED; for some of those events, the FRICAT M_L values are slightly lower than those computed by the SED. In Fig. 8a we compare the magnitude distribution of the events detected by the national network of the SED over the period 1972–2013 in the Fribourg region (Fäh et al. 2011) with the magnitude distribution of the Fribourg clusters identified in this study. The higher-magnitude sequences of 1987, 1995, and 1999 on the FL are well imaged within a rather continuous distribution of M_L 2 events. Starting in 2009, the higher detection rate by the SED seen in Fig. 8a corresponds to the installation of stations SCOU and STAF on the FL (see Fig. 2). The temporal evolution in the period 2009–2013 of the seismic activity in the Fribourg region is pictured by the magnitude-time distribution of the five earthquake families derived by the cross-correlation analysis (Fig. 8b): it is characterized by a fairly constant background seismicity in the $-0.5 < M_L < 0.5$ range,

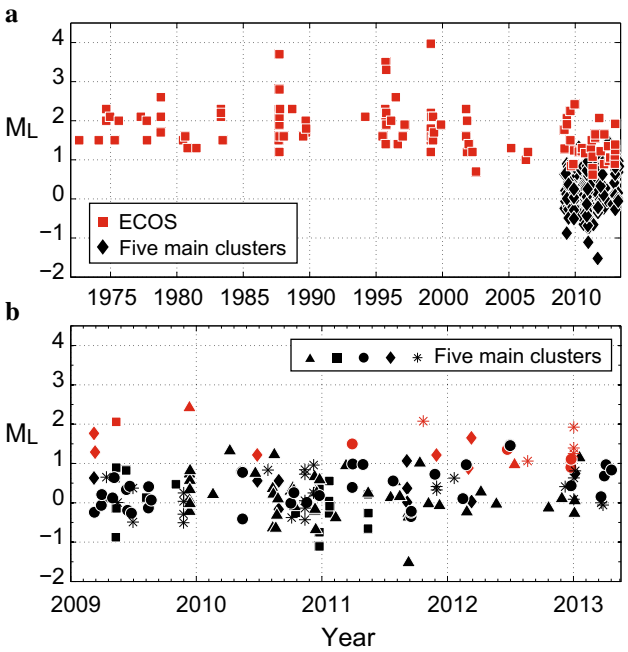

Fig. 8 **a** Temporal evolution of the seismic activity in Fribourg region between 1972 and 2013 (*squares*, ECOS (Fäh et al. 2011) and data archives of the SED) compared to the time distribution of the five main clusters along the FL and the Fribourg Cluster (*diamonds*). **b** M_L-time distribution of the five main clusters derived from the linkage analysis (see legend in Fig. 7)

punctuated by a few more energetic $M_L \sim 2.0$ sequences. Such a pattern of low-magnitude seismic activity fits a model where the overall shear is partitioned over small-scale ($\sim$10–100 m) ruptures.

3.5 Summary of the microseismic observations

The results of the microseismic investigations undertaken in the context of the present study can be summarized as follows:

- The systematic sonogram scans of the continuous data recorded at three stations of the SED and at the two temporary SNS arrays successfully lowered the event detection threshold by about one magnitude unit compared to traditional monitoring techniques (Vouillamoz et al. 2016).
- Based partly on absolute locations and partly on association by signal similarity, most of the additional low-magnitude events recorded over the 4-year period between 2009 and 2013 are associated with a small cluster below the city of Fribourg (the so-called Fribourg cluster) as well as with different segments of the N–S striking Fribourg Lineament, FL, to the east of the city of Fribourg, the latter having been active already previously.
- Both the absolute locations and the event classification based on waveform similarities of the additional low-magnitude events are compatible with earlier focal depth estimates that indicate that the Fribourg earthquakes appear to be generated exclusively at shallow depths in the sedimentary cover; thus, there is no evidence in the analyzed dataset for seismic activity in the basement.

4 Structural model of the Fribourg region

Newly reinterpreted seismic data (Interoil 2010) were used to derive a 3D fault model in the Fribourg region and more specifically along the FL fault system, and were combined with results from recent studies on fractures observed at the surface.

4.1 Subsurface data

Based on 440 km of oil industry seismic profiles and calibrated on deep borehole data, Interoil (2010) interpolated fault zones between different seismic lines and produced structural maps over five stratigraphic horizons: base Mesozoic, top Muschelkalk (Middle Triassic), top Lias (Lower Jurassic), base Malm (Upper Jurassic), and base Tertiary (Fig. 9a, b). In transects across the FL, gentle folding, as well as near vertical fault zones rooting in the basal decollement in the middle and upper Triassic evaporites are well imaged in the Mesozoic layers (Fig. 9b). The quality of the seismic data, as well as the absence of continuous seismic reflectors impedes a clear imaging of structures in the basement as well as in the Tertiary mostly detrital cover series. However, no clear offset in the basement and no evidence for throughgoing faults can be found. Rather offsets are restricted to the Mesozoic–Cenozoic sedimentary cover. Thickening of the Middle Triassic formation underneath the FL fault zone is associated with evaporite migration and may be linked to the development of the steep faults that are subsequently reactivated as tear faults in the present stress field. These arguments support a decoupling between the fault zones imaged in the sedimentary strata and potential tectonic features located in the basement.

The five structural map horizons by Interoil (2010) were combined to interpolate 3D fault plane surfaces using ArcGIS 3D Analyst™ (Fig. 9c). The 3D fault planes were subsequently projected to the topographic surface by extrapolating series of predefined control points on each fault segment across each stratigraphic horizon (Vouillamoz 2015). For the first time, the intersection of the fault planes with the topography was checked for correspondence with known faults and/or visible lineaments on a high resolution digital elevation model (swissAlti3D DEM© swisstopo). The new fault model shows that the northward extension of the faults located east of the city of Fribourg and pertaining to the FL, ends to the North at about the latitude of the city of Bern (Fig. 9c). The model displays two main N–S trending fault zones along strike of the FL: the Fendringen structure to the north and the St. Sylvester structure in the south (Fig. 9c). Since the seismic line grid is unevenly distributed around the city of Fribourg, no specific subsurface tectonic features are interpreted there (Fig. 9a).

4.2 Surface data

Given the important Quaternary deposits, structural data are unevenly distributed within the study area and mostly limited to incised river valleys (Fig. 10a). Various mesoscale brittle tectonic structures such as faults, brittle deformation bands, slickensides, and joints are reported in the Molasse sediments outcrops (GA25: Geological Atlas of Switzerland at the scale 1:25′000, swisstopo; Ibele 2011; Matzenauer 2012) and it can be shown that broad undeformed areas alternate with rather restricted strongly deformed zones (Ibele 2011). Strong lateral variations of facies within the Tertiary sediments (shales, clayey sands and sandstones) influence the fault style, which ranges from clayey cataclasite in clayey sands (Fig. 10b) to dense

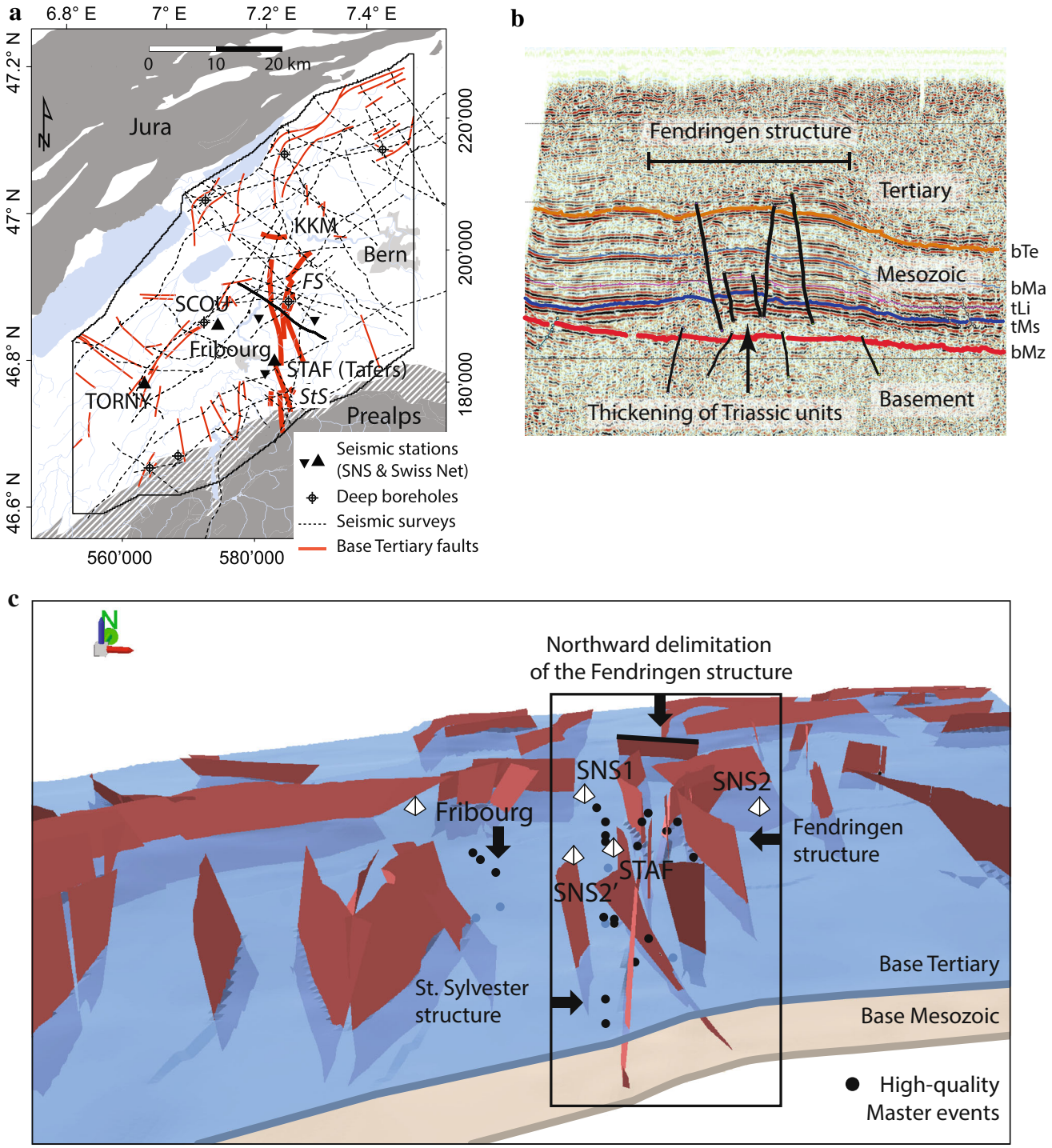

Fig. 9 **a** Base Tertiary horizon structural map by (Interoil 2010) (*bold lines*) with traces of interpreted seismic profiles (*dotted lines*) and location of deep boreholes used for calibration (*tagged circles*). **b** Seismic transect FR.N8105 across the FL (see *trace* of *line* in **a**); five stratigraphic limits were interpreted and interpolated in structural map horizons: *bMz* base Mesozoic, *tMs* top Muschelkalk, *tLi* top Lias, *bMa* base Malm, *bTe* base Tertiary (Interoil 2010). **c** 3D fault plane model of Fribourg region with interpolated base Mesozoic and base Tertiary horizons. The spatial distribution of well constrained master event hypocenters of the Fribourg micro-earthquake dataset is shown and correlates well with the Fendringen and St. Sylvester structures (FS and StS, respectively in **a**). Due to the absence of seismic survey in Fribourg agglomeration, no subsurface tectonic features that could be linked to the Fribourg Cluster are interpreted at that location

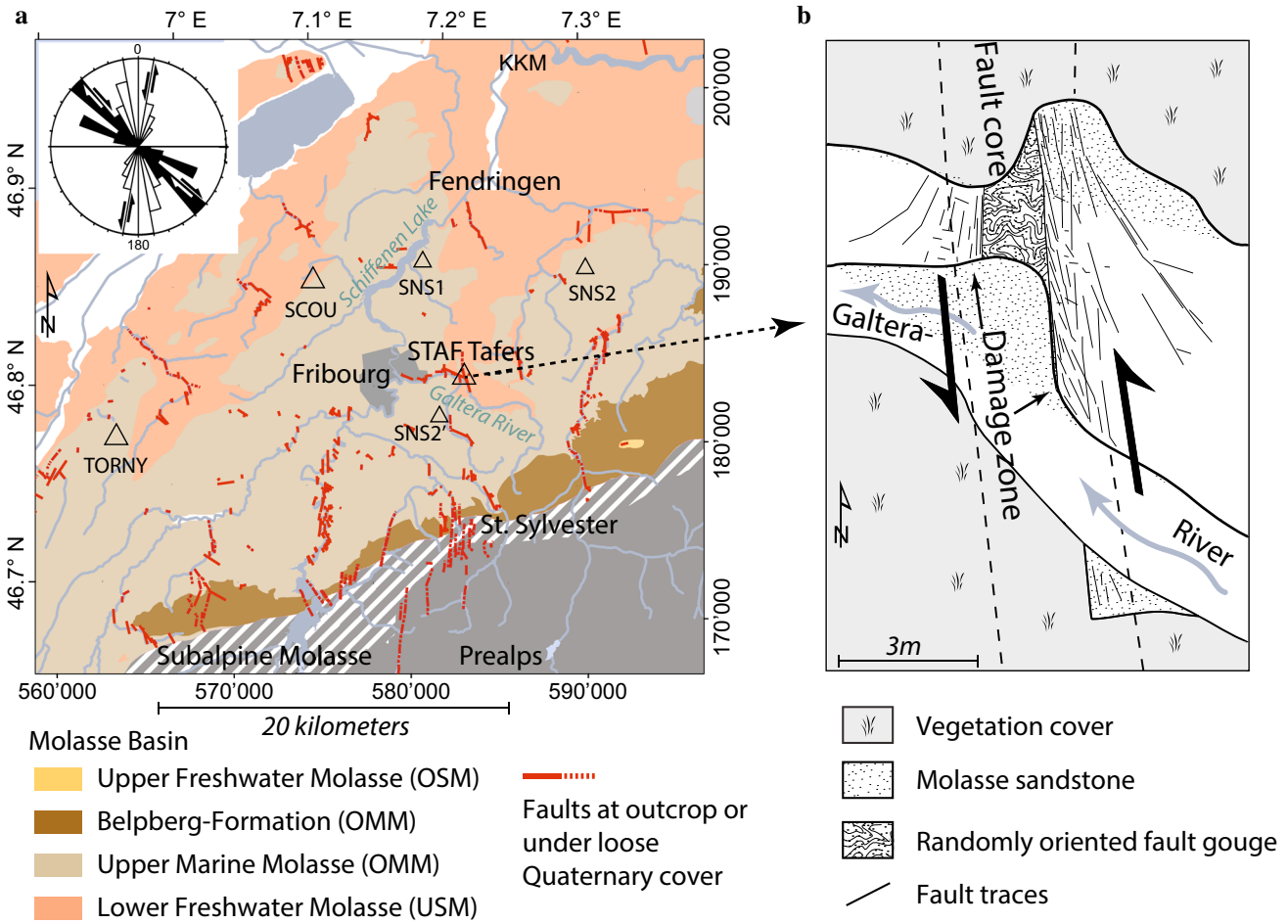

Fig. 10 **a** Geological map of the study area with observed fault distribution (Source: GA25; Ibele 2011; Matzenauer 2012; Vouillamoz 2015). Strikes of mapped fault zones are indicated in the *upper left rose diagram* (dextral in *black* and sinistral in *white*) (Ibele 2011). **b** Sketch of a larger discrete fault at Tafers (location of STAF

fracture networks in sandstones. The rheological change associated to lateral facies variations acts like a mechanical barrier for discrete fault propagation, and a maximum fault length of 1–3 km in the Tertiary units of the Molasse basin can be estimated. Mapped fault zones feature a general *en-échelon* arrangement, and the largest discrete fault zone within the study area is reported near Tafers (STAF receiver site) in the Galtera river bed (Fig. 10b). It represents a 1–1.5 m wide core zone of randomly oriented fault gouge and a several meters wide damage zone on either side of the fault (Ibele 2011). At the St. Sylvester location, faults are apparent in the geomorphology with up to 700 m left-lateral offsets observed in the Subalpine Molasse units. Northward, faults are mapped along strike of two N–S flowing streams at Fendringen (Ibele 2011) (Fig. 10a). The St. Sylvester, Tafers and Fendringen fault zones correlate along strike with the FL, and we consider them to be the surface expression of the active fault zones at depth.

Kinematic indicators show left-lateral motion on subvertical faults oriented N–S to NNE–SSW and right-lateral movement on faults oriented NW–SE to WNW–ESE. This conjugate fault system is consistent with stress data derived from faults and striation which show a rather uniform NW–SE directed compressive stress field and a NE–SW oriented extension (Ibele 2011) (Fig. 10a). This stress field is compatible with the present day stress state in the Alpine foreland of northwestern Switzerland derived from earthquake data (Kastrup et al. 2004).

5 Integrated model of the Fribourg Lineament

Despite the sparse surface data it is possible to identify a discrete fault zone at the Tafers location (Fig. 10) (Ibele 2011). Combined with the interpretation from seismic lines, we consider that the Fendringen and St. Sylvester structure constitute a continuous damage zone that consists of *en-échelon* arranged fault segments with moderate lateral extent (<5 km) and that cross-cuts the detached Tertiary and Mesozoic cover series and roots in the basal

middle–upper Triassic evaporites (Fig. 9b). Seismic imaging and structural data are integrated with earthquake data on a synthetic cross-section oriented N–S along the FL (Fig. 11). The inferred fault zone surface is schematically projected and pictured on the profile by shaded area (Fig. 11a). Solid contours display regions constrained by seismic data, whereas dotted contours indicate the extrapolated surfaces dimension. Dashed lines below the topography point out locations where fault zones have been measured in Tertiary outcrops. The length of the inferred fault zone reaches about 30 km at the surface and at the base of the Tertiary layers, and some 20 km at the base of the Mesozoic series.

Potentially active seismic zones along the FL are evaluated using reliable features of four reference events (i.e. the highest magnitude event among each earthquake family derived from the waveform cross-correlation analysis along the FL) (Table 1). Note that because of its offset to the West, the Fribourg cluster is not included in this analysis. The source location of each reference events is evaluated with S–P travel-time differences recorded at STAF. Using a half-space v_p velocity model of 4.5 km/s and a v_p/v_S ratio

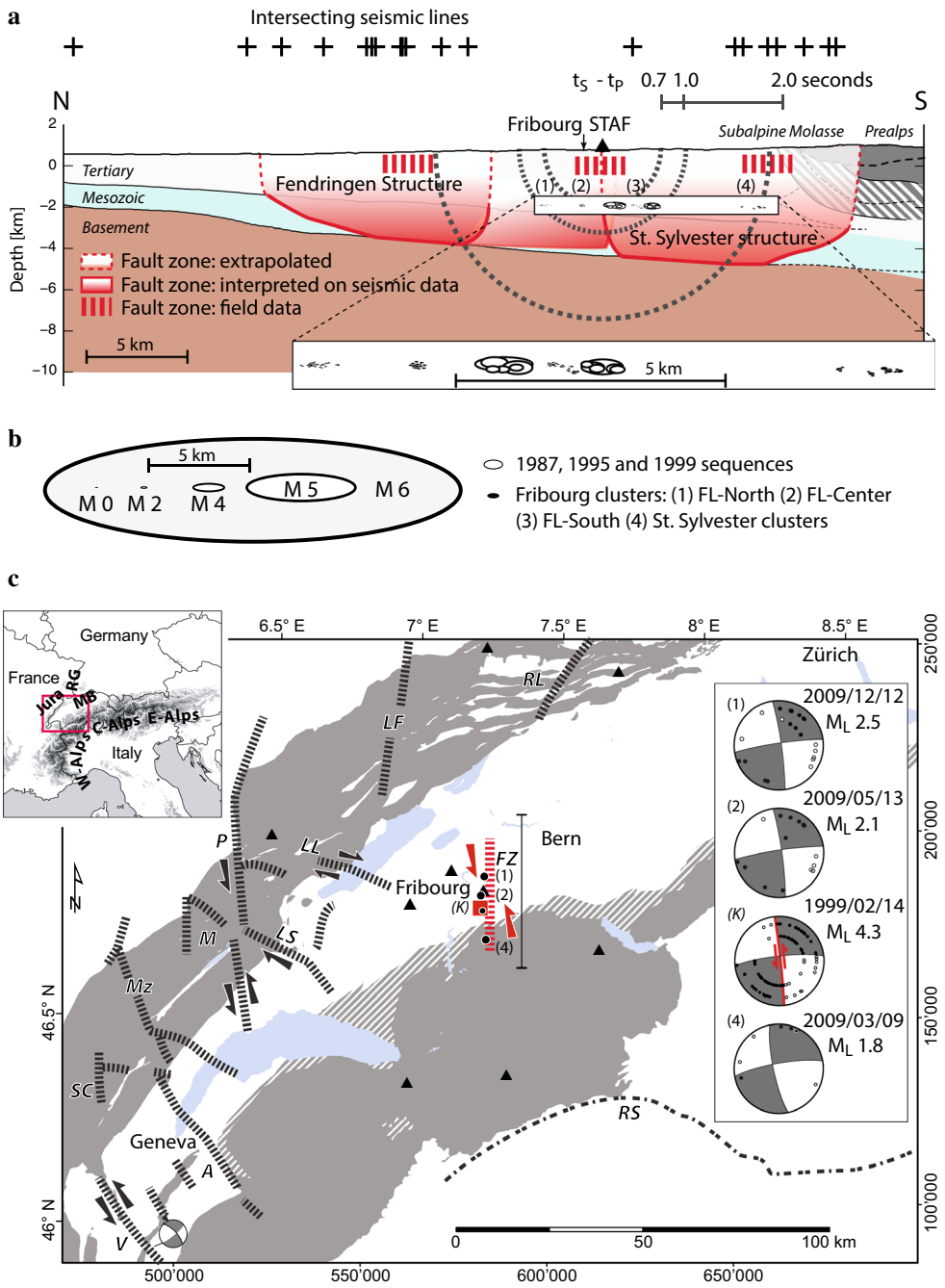

Fig. 11 **a** Schematic profile on the FL (N 168′000–N 202′000 in CH1903-LV03 projection system, see trace in **c**) that integrates geological, seismic imaging and earthquake data at scale. **b** Estimated rupture surfaces for **M** 0 to **M** 6 earthquakes, using the same scaling as in **a**. Scaling relationships are excerpted from Bohnhoff et al. (2010) and Fagereng and Toy (2011). **c** Regional tectonic map featuring the major fault systems in the Alpine foreland across the Jura belt and the western Swiss Molasse basin: *V* Vuache, *SC* St-Claude, *A* Arve, *Mz* Morez, *M* Mouthe, *LS* la Sarraz, *P* Pontarlier, *LL* la Lance, *LF* la Ferrière, *F* Fribourg (Fendringen and St. Sylvester); and RL, Rhenish Lineament [modified from Chevalier et al. (2010)]. RS indicates the Rhône-Simplon Accident. *Left frame*: the focal mechanisms computed for three of the reference events (1, 2, and 4) (Deichmann et al. 2010; Vouillamoz, 2015) are consistent with the well constrained fault plane solutions computed for the M_L 4.3 event on the FL (Kastrup et al. 2007) and suggest almost pure strike-slip rupture along N–S oriented fault planes

Table 1 Reference events on the Fribourg Lineament

Cluster	Date	Time (UTC)	Lat/Lon (°)	X/Y/Z (m)	M_L	STAF t_S–t_P (s)	Rel. t_S–t_P (s)	FM
(1) FL-North	2009.12.12	00:17:50	46.841/7.220	583,326/187,771/−1280	2.4	0.9	0.2	Yes
(2) FL-Center	2009.05.13	04:07:20	46.800/7.209	582,496/183,275/−2980	2.1	0.7	0.1	Yes
(3) FL-South	2011.03.29	22:13:50	46.768/7.214	582,898/179,690/−1580	1.5	0.8	0.2	No
(4) St. Sylvester	2009.03.09	16:30:30	46.707/7.225	583,686/172,853/−1480	1.8	2.0	0.4	Yes

Cluster, main clusters on the FL; date, date of reference event; time, UTC time of reference event; lat/lon, latitude and longitude of reference event; X/Y/Z, hypocenter location by HypoLine software (Joswig 2008; Vouillamoz et al. 2016) in the CH1903-LV03 projection system; M_L, local magnitude (Vouillamoz et al. 2016); STAF t_S–t_P, S–P travel-time differences of reference event picked at station STAF; rel. t_S–t_P, maximum relative S–P travel-time difference observed between the reference event and the clustered events; FM, focal mechanism [solutions published in Deichmann et al. (2010) for event (1) and (2) and in (Vouillamoz 2015) for event (4)]

of 2.0 suited for sedimentary rocks, observed S–P travel-time differences of 0.7–2.0 s (Fig. 5d; Table 1) correspond to receiver-source distances of 2.8–8.1 km that are represented on the profile by dotted semi-circles centered on STAF (Fig. 11a). An estimated focal depth of about 2 km is attributed to each reference event, in agreement with the focal depth constrained by synthetic waveform modelling (Kastrup et al. 2007) (see Sect. 3.1). The four reference events are represented on the profile by scaled rupture surface ellipses. The lower-magnitude events of the FRICAT dataset that were associated to the four reference events by the waveform similarity analysis (see Sect. 3.3) are then schematically projected based on observed S–P travel-time differences relative to the master events (Table 1). The sequences of 1987, 1995 and 1999 are projected using the relative location by Kastrup et al. (2007). The scaled rupture size of the events is estimated following Bohnhoff et al. (2010) and Fagereng and Toy (2011), and considering $-1.5 < M_L < 0.5$ as **M** 0, $0.5 < M_L < 1.5$ as **M** 1, $1.5 < M_L < 2.5$ as **M** 2, $2.5 < M_L < 3.5$ as **M** 3 and $3.5 < M_L < 4.5$ as **M** 4 (Fig. 11b). Thus, a **M** 0 earthquake corresponds to a dot on the profile. The final cross-section highlights the size of potential active fault zones along the FL.

6 Discussion

Tear faults in the Molasse basin and the Jura fold-and-thrust belt show directions that may be considered as inherited from basement structures as is the case for the St. Gallen graben/strike-slip fault zone in eastern Switzerland (e.g. Heuberger et al. 2016), or the Freiburg–Bonndorf–Bodensee fault in the Hegau area (e.g. Egli et al. 2016). Unlike in eastern Switzerland, where these faults presently reach from the basement into the sedimentary cover, in western Switzerland the large tear faults (e.g. the Pontarlier and the Vuache faults, Fig. 11c) are in the detached sedimentary cover only. Here, the western Alpine foreland (Molasse basin and Jura fold-and-thrust belt) is displaced as much as 25–30 km towards the NW along the basal decollement in a wedge-top geodynamic setting (Sommaruga et al. 2012 and references therein).

Using geological data and subsurface imaging, the tectonic structure related to the FL is interpreted as a N–S oriented *en-échelon* fault zone of moderate lateral extent (<5 km), made of series of fault strings that reach a cumulated length of some 30 km in the detached sedimentary cover east of the city of Fribourg, and which terminate northward at about the latitude of the city of Bern (Fig. 9). Therefore, the Fribourg zone is not related, at least in shallow layers, to the Rhenish Lineament as suggested in previous studies (Allenbach and Wetzel 2006; Kastrup et al. 2007; Chevalier et al. 2010). Considering the general high uncertainties linked to interpretations of basement structures in the existing seismic reflection datasets across the western Swiss Molasse basin (Interoil 2010; Meier 2010; Sommaruga et al. 2012), we do not conclude anything about a potential major crustal feature that would link the Rhenish lineament (Allenbach and Wetzel 2006) to potential basement structures below the FL. Rather, we suggest that the FL is comparable in its tectonic setting to the Vuache fault zone which triggered in 1996 a M_L 5.3 earthquake in the sedimentary cover (1–3 km depth) with left-lateral strike-slip mechanism (Fig. 11c) (Thouvenot et al. 1998; Courboulex et al. 1999; Baize et al. 2011).

Studies on the regional seismicity in the northern Alpine foreland have shown that many detected earthquakes are located in the basement (e.g. Singer et al. 2014). However, these studies refer to an area where the alpine foreland is in a purely flexural foreland context and do not apply further west. In the western wedge-top foreland, most earthquakes are located in the detached sedimentary cover. This does not exclude earthquakes from occurring in the basement, but rather point to a more complex strain/stress partitioning due to multiple detachments along two major decollements at the base of the Mesozoic cover series and at the base of the tertiary Molasse sediments in the meridional parts of the foreland basin. In both domains (cover and basement), the focal mechanisms are dominantly strike-slip along two

major N–S and NW–SE directions, i.e. where the principal stress S1 is horizontal and shows a counterclockwise rotation in the NW quadrant (Kastrup et al. 2004).

We find clear evidence for clustered microseismic activity in the period 2009–2013 over a length of about 11 km in the sedimentary cover beneath STAF (Fig. 11a). Predicted distances by S–P travel-time differences recorded at STAF show that the St. Sylvester cluster (4), which is the southernmost cluster, lies most likely in the Molasse basin (Fig. 11a), and not in the Prealps, as it appears on epicenter map (Figs. 3, 7). Therefore, it is inferred that the four main earthquake families resolved by the waveform similarity analysis correspond to on-going seismic activity in restricted zones of the FL. Since a focal depth of 2 km projects close to the Tertiary (Cenozoic)–Mesozoic series boundary, it is not possible to discriminate conclusively if the events are restricted to the Tertiary cover (Molasse units) or to the underlying Mesozoic sequences, or possibly distributed over both. In the seismic atlas of the Molasse basin, Sommaruga et al. (2012) report that there is not always a clear evidence for linking fault zones interpreted in the Tertiary series with the ones observed in the underlying Mesozoic units. In addition, the authors suggest that Tertiary sediments are folded independently from underlying strata, thus requiring a secondary detachment horizon near the base Tertiary. In this scenario, also suggested based on analogue modeling (Bonnet et al. 2007), and if the Fribourg events could be assigned to the Tertiary cover, the potential size for an earthquake to be generated along the FL would be reduced. However, given the uncertainty in depth location, the available data do not justify such a conclusion.

In Fig. 11c, we reproduce the fault-plane solutions for the 2009/05/13 (cluster 2) and 2009/12/12 (cluster 1) reference events from Deichmann et al. (2010). The focal mechanisms correspond to almost pure strike-slip and are very similar to the well-constrained focal mechanism of the 1999/02/14, M 4 event, for which the N–S striking focal plane with left-lateral slip could be identified as the active fault plane (Kastrup et al. 2007). An additional focal mechanism was computed for the St-Sylvester 2009/03/09 reference event (cluster 4) using seven onset polarities (Fig. 11c). Although the fault-plane solution is not well constrained, it is consistent with the other ones. Individual fault-plane solutions of the other events detected over the period 2009–2013 could not be constructed due to their small magnitudes. However, from the signal character of the events along the FL recorded at station STAF we can conclude that most likely their mechanisms are similar to those of the larger events. In fact, in a direction that coincides with the strike of one of the possible fault planes, the P-waves radiated by a shear dislocation are weak and emergent, while the S-waves are strong and impulsive. Moreover, small variations in strike or dip of the fault plane can cause a polarity reversal of the observed P-onset. This is precisely what is seen in practically all the signals of the events along the FL recorded at STAF (Figs. 5c, d, 6d). Given the location of STAF on the trace of the FL, as outlined by the N–S oriented earthquake epicenters, the observed signal character is consistent with the conclusion that rupture along the various segments of the FL occurs as left-lateral slip on N–S oriented near-vertical fault planes.

In the near vicinity of the dam of the Schiffenen (Fig. 10) several sulfur-rich cold water sources are known. The origin of sulfur enrichment is related to the gypsum and dolomite rich layers of the USM formed from evaporitic lake waters (Platt 1992). Thus, these sources may indicate facilitated fluid circulation along fault systems, which act as links to the surface. Hydraulically conductive faults are known to be critically stressed faults (Townend and Zoback 2000) supporting the idea of active fluid conduits between surface and the seismically activated zones at the base of the Tertiary Molasse sediments along the fault zone. In addition, but also in general, excess water loads may act as a trigger on a critically stressed fault system and thus induce earthquake swarms. Although, the present data record for our study area, is too sparse and incomplete to make a plausible correlation, this has been postulated elsewhere in the Alps (von Hagke et al. 2014 and references therein). Similar situations of induced seismicity can also be linked to excess rainfall and flooding, as known in other regions in Switzerland and southeastern Germany (e.g. Kraft et al. 2006; Husen et al. 2007). One can thus consider that the Alpine orogenic wedge is close to failure and that faults are critically stressed.

That the deformation due to the NW–SE directed compression of the northwestern Alpine foreland of Switzerland (Kastrup et al. 2004) manifests itself as slip on favorably oriented strike-slip/tear faults rather than on favorably oriented thrust/reverse faults is due to the fact that the differential stress needed to activate a thrust fault is significantly higher than for a more or less vertical strike-slip fault at the same depth (Sibson 1974; Zoback 2007). Thus the existence and repeated rupture of favorably oriented critically stressed tear faults, such as the N–S oriented fault segments that constitute the FL, sets a limit to the magnitude of the ambient differential stress. As a consequence, the differential stress cannot reach a sufficiently high level to activate any possibly well-oriented reverse faults. According to the cumulative size of the seismically active zones along the FL and the anastomosing tendency of *en-échelon* fault zones, we infer the potential for a **M** 5 earthquake to be generated in the sedimentary cover along the FL, similar to the Annecy earthquake on the Vuache fault in 1996, mentioned above. If, in addition, we allow an earthquake to rupture the

presently active segments of the FL as well as its northward extension along the Fendringen structure, then we cannot exclude the possibility of a higher-magnitude event, even without invoking an undiscovered fault that extend into the basement (Fig. 11a, b). Thus, the FL constitutes a significant seismic hazard in the Swiss alpine foreland and deserves continued seismic monitoring.

Acknowledgements This work was financially supported by the RESUN AG (REmplacement SUisse Nucléaire, Swiss nuclear replacement) and the BKW (Bernische Kraftwerke, the power supply company of the canton Bern in Switzerland) (Project number: R49000048 KB). Interoil E&P Switzerland AG and the Nagra (Swiss National Cooperative for the Disposal of Radioactive Waste) are thanked for sharing interpreted seismic data; swisstopo is thanked for giving access to the Swiss GIS archives. The authors are grateful to Gilles Hillel Wust-Bloch (University of Tel-Aviv) who co-initiated this work, for fruitful discussion and constructive criticism. The authors thank Martinus Abednego (University of Fribourg), for developing codes to interpolate the 3D fault model, and Eva Matzenauer (swisstopo) who created the early version of the GIS database presented in this paper. We are grateful to the guest-editor Christian Sue and two anonymous reviewers, for their constructive comments that improved the manuscript.

References

Abednego, M. (2016). *Microseismic tomography analysis of the larger Fribourg area (western Swiss Molasse Basin)*. Ph.D. dissertation, GeoFocus 40, University of Fribourg, Fribourg, Switzerland.

Allenbach, R. P., & Wetzel, A. (2006). Spatial patterns of Mesozoic facies relationships and the age of the Rhenish Lineament: A compilation. *International Journal of Earth Sciences (Geologische Rundschau), 95*(5), 803–813. doi:10.1007/s00531-006-0071-0.

Augliera, P., Cattaneo, M., & Eva, C. (1995). Seismic multiplets analysis and its implication in seismotectonics. *Tectonophysics, 248,* 219–235.

Baize, S., Cushing, M., Lemeille, F., Gelis, C., Texier, D., Nicoud, G., et al. (2011). Contribution to the seismic hazard assessment of a slow active faut, the Vuache fault in the southern Molasse basin (France). *Bulletin de la Société Géologique de France, 182*(4), 347–365.

Barani, S., Ferretti, G., Massa, M., & Spallarossa, D. (2007). The waveform similarity approach to identify dependent events in instrumental seismic catalogues. *Geophysical Journal International, 168*(1), 100–108. doi:10.1111/j.1365-246X.2006.03207.x.

Berger, Z., & Gundlach, T. (1990). The contribution of satellite interpretation to exploration in west Germany and Switzerland: BEB. Task Force Exploration strategy, Report No. 3.

Bohnhoff, M., Dresen, G., Ellsworth, W. L., & Ito, H. (2010). Passive seismic monitoring of natural and induced earthquakes: Case studies, future directions and socio-economic relevance. In S. Cloetingh & J. Negendank (Eds.), *New frontiers in integrated solid earth sciences: International year of planet earth* (pp. 261–285). Dordrecht: Springer Science + Business Media B.V.

Bonnet, C., Malavieille, J., & Mosar, J. (2007). Interactions between tectonics, erosion, and sedimentation during the recent evolution of the Alpine orogen: Analogue modeling insights. *Tectonics, 26,* TC6016. doi:10.1029/2006TC002048.

Burkhard, M. (1990). Aspects of the large-scale Miocene deformation in the most external part of the Swiss Alps (Subalpine Molasse). *Eclogae Geologicae Helvetiae, 83*(3), 559–583.

Burkhard, M., & Sommaruga, A. (1998). Evolution of the western Swiss Molasse basin: Structural relations with the Alps and the Jura belt. In A. Mascle, C. Puigdefàbregas, H. P. Luterbacher, & M. Fernàndez (Eds.), *Cenozoic foreland basins of Western Europe* (pp. 279–298). London: Geological Society Special Publications, 134.

Buxtorf, A. (1907). Zur Tektonik des Kettenjura. *Bericht der Versammlung des Oberrheinischen Geologischen Vereins, 40,* 70–111.

Cattaneo, M., Augliera, P., Spallarossa, D., & Lanza, V. (1999). A waveform similarity approach to investigate seismicity patterns. *Natural Hazards, 19,* 123–128.

Cederbom, C. E., van der Beek, P., Schlunegger, F., Sinclair, H. D., & Oncken, O. (2011). Rapid extensive erosion of the North Alpine foreland basin at 5–4 Ma. *Basin Research, 23*(5), 528–550. doi:10.1111/j.1365-2117.2011.00501.x.

Chevalier, G., Diamond, L. W., & Leu, W. (2010). Potential for deep geological sequestration of CO_2 in Switzerland: A first appraisal. *Swiss Journal of Geosciences, 103*(3), 427–455. doi:10.1007/s00015-010-0030-4.

Courboulex, F., Deichmann, N., & Gariel, J. (1999). Rupture complexity of a moderate intraplate earthquake in the Alps: the 1996 M5 Epagny–Annecy earthquake. *Geophysical Journal International, 139,* 152–160.

Deichmann, N., Clinton, J., Husen, S., Edwards, B., Haslinger, F., Fäh, D., et al. (2010). Earthquakes in Switzerland and surrounding regions during 2009. *Swiss Journal of Geosciences, 103*(3), 535–549. doi:10.1007/s00015-010-0039-8.

Deichmann, N., & Garcia-Fernandez, M. (1992). Rupture geometry from high-precision relative hypocenter locations of microearthquake clusters. *Geophysical Journal International, 110,* 501–517.

Diehl, T., Deichmann, N., Clinton, J., Kästli, P., Cauzzi, C., Kraft, T., et al. (2015). Earthquakes in Switzerland and surrounding regions during 2014. *Swiss Journal of Geosciences, 108*(2–3), 425–443. doi:10.1007/s00015-015-0204-1.

Egli, D., Mosar, J., Ibele, T., & Madritsch, H. (2016). The role of precursory structures on Tertiary deformation in the Black Forest—Hegau region. *International Journal of Earth Sciences (Geologische Rundschau).* doi:10.1007/s00531-016-1427-8.

Fagereng, A., & Toy, V. G. (2011). Geology of the earthquake source: An introduction. *Geological Society, London, Special Publications, 359*(1), 1–16. doi:10.1144/SP359.1.

Fäh, D., Giardini, D., Bay, F., Bernardi, F., Braunmiller, J., Deichmann, N., et al. (2003). Earthquake Catalogue of Switzerland (ECOS) and the related macroseismic database. *Eclogae Geologicae Helvetiae, 96,* 219–236.

Fäh, D., Giardini, D., Kästli, P., Deichmann, N., Gisler, M., Schwartz-Zanetti, G., Alvare-Rubio, S., Sellami, S., Edwards, B., Allmann, B., Bethmann, F., Woessner, J., Gassner-Stamm, G., Fritsche, S., Eberhard, D. (2011). ECOS-09 Earthquake Catalogue of Switzerland Release 2011. Report and Database, Public catalogue, 17.4.2011.

Heuberger, S., Roth, P., Zingg, O., Naef, H., & Meier, B. P. (2016). The St. Gallen Fault Zone: a long-lived, multiphase structure in

the North Alpine Foreland Basin revealed by 3D seismic data. *Swiss Journal of Geosciences, 109*(1), 83–102. doi:10.1007/s00015-016-0208-5.

Homewood, P., Allen, P. A., & Williams, G. D. (1986). Dynamics of the Molasse Basin of Western Switzerland. In P. A. Allen & P. Homewood (Eds.), *Foreland basins* (pp. 199–217). Oxford: Blackwell Publishing Ltd.

Husen, S., Bachmann, C. E., & Giardini, D. (2007). Locally triggered seismicity in the central Swiss Alps following the large rainfall event of August 2005. *Geophysical Journal International, 171*(3), 1126–1134. doi:10.1111/j.1365-246X.2007.03561.x.

Husen, S., Kissling, E., Deichmann, N., Wiemer, S., Giardini, D., & Baer, M. (2003). Probabilistic earthquake location in complex three-dimensional velocity models: Application to Switzerland. *Journal of Geophysical Research, 108*(B2), ESE 5. doi:10.1029/2002JB001778.

Ibele, T. (2011). *Tectonics of the western Swiss Molasse basin during Cenozoic time*. Ph.D. dissertation, GeoFocus 27, University of Fribourg, Fribourg, Switzerland.

Interoil. (2010). *2D Seismic Interpretation in den Gebieten Payerne, Fribourg und Berner Seeland*. Zürich: Bericht vorbereitet von Interoil E&P Switzerland AG für die RESUN AG.

Jordi, A. (1951). Zur Stratgraphie und Tektonik der Molasse von Yverdon. *Bulletin der Vereinigung Schweiz, Petroleum-Geologen und Ingenieure, 18*(55), 1–14.

Joswig, M. (2008). Nanoseismic monitoring fills the gap between microseismic networks and passive seismic. *First Break, 26,* 117–124.

Kastrup, U., Deichmann, N., Fröhlich, A., & Giardini, D. (2007). Evidence for an active fault below the northwestern Alpine foreland of Switzerland. *Geophysical Journal International, 169*(3), 1273–1288. doi:10.1111/j.1365-246X.2007.03413.x.

Kastrup, U., Zoback, M. L., Deichmann, N., Evans, K. F., Giardini, D., & Michael, A. J. (2004). Stress field variations in the Swiss Alps and the northern Alpine foreland derived from inversion of fault plane solutions. *Journal of Geophysical Research, 109*(B1), B01402. doi:10.1029/2003JB002550.

Kraft, T., & Deichmann, N. (2014). High-precision relocation and focal mechanism of the injection-induced seismicity at the Basel EGS. *Geothermics, 52,* 59–73. doi:10.1016/j.geothermics.2014.05.014.

Kraft, T., Wassermann, J., Schmedes, E., & Igel, H. (2006). Meteorological triggering of earthquake swarms at Mt. Hochstaufen, SE-Germany. *Tectonophysics, 424,* 245–258. doi:10.1016/j.tecto.2006.03.044.

Laubscher, H. P. (1961). Die Fernshubhypothese der Jurafaltung. *Eclogae Geologicae Helvetiae, 54,* 221–282.

Laubscher, H. P. (1987). Die Tektonische Entwicklung der Nordschweiz. *Eclogae Geologicae Helvetiae, 80*(2), 287–303.

Laubscher, H. P. (1997). The decollement hypothesis of Jura folding after 90 years. *Swiss Bulletin for Applied Geology, 2*(2), 167–182.

Massa, M., Eva, E., Spallarossa, D., & Eva, C. (2006). Detection of earthquake clusters on the basis of waveform similarity: An application in the monferrato region (Piedmont, Italy). *Journal of Seismology, 10*(1), 1–22. doi:10.1007/s10950-006-2840-4.

Matzenauer, E. (2012). *Tectonics of the Préalpes Klippen and the Subalpine Molasse (Canton Fribourg, Switzerland)*. Ph.D. dissertation, GeoFocus 31, University of Fribourg, Fribourg, Switzerland.

Meier, B.P. (2010). Ergänzende Interpretation reflexionsseismischer Linien zwischen dem östlichen und westlichen Molassebecken—Gebiete Waadtland Nord, Fribourg, Berner Seeland und Jurasüdfuss zwischen Biel und Oensingen: Nagra Interner Bericht, NIB 09-09, Baden, Switzerland.

Naef, H., Diebold, P., & Schlanke, S. (1985). Sedimentation und Tektonik im Tertiär der Nordschweiz. Nagra Technischer Bericht, NTB 85-14, Baden, Switzerland.

Nagra. (1988). Möglichkeiten zur Endlagerung langlebiger radioaktiver Abfälle in den Sedimenten der Schweiz: Sedimentstudie Zwischenbericht. Nagra Technical Report, NTB 88-25, Baden, Switzerland.

Plancherel, R. (1996). Tektonische Karte Blatt Fribourg (1185). *Geologischer Atlas der Schweiz 1:25 000 (GA 25)—Atlas géologique de la Suisse 1:25 000*, swisstopo.

Platt, N. H. (1992). Fresh-water carbonates from the Lower Freshwater Molasse (Oligocene, western Switzerland): Sedimentology and stable isotopes. *Sedimentary Geology, 78,* 81–89.

Scarfì, L., Langer, H., & Gresta, S. (2003). High-precision relative locations of two microearthquake clusters in Southeastern Sicily, Italy. *Bulletin of the Seismological Society of America, 93*(4), 1479–1497.

Schlunegger, F., & Kissling, E. (2015). Slab rollback orogeny in the Alps and evolution of the Swiss Molasse basin. *Nature Communications, 6,* 8605. doi:10.1038/ncomms9605.

Schuppli, H. M. (1950). Erdölgeologische Untersuchungen in der Schweiz III, Teil 8. Abschnitt. Ölgeologische Untersuchungen im Schweizer Mittelland zwischen Solthurn und Moudon. *Bulletin der Vereinigung Schweiz, Petroleum-Geologen und Ingenieure, 52*(17), 51–53.

Sibson, R. H. (1974). Frictional constraints on thrust, wrench and normal faults. *Nature, 249*(5457), 542–544. doi:10.1038/249542a0.

Sick, B., Walter, M., & Joswig, M. (2014). Visual event screening of continuous seismic data by supersonograms. *Pure and Applied Geophysics, 171*(3), 549–559. doi:10.1007/s00024-012-0618-x.

Singer, J., Diehl, T., Husen, S., Kissling, E., & Duretz, T. (2014). Alpine lithosphere slab rollback causing lower crustal seismicity in northern foreland. *Earth and Planetary Science Letters, 397,* 42–56. doi:10.1016/j.epsl.2014.04.002.

Sommaruga, A. (1995). Tectonics of the central Jura and the Molasse basin New insights from the interpretation of seismic reflection data. *Bulletin de la Société Neuchâteloise des Sciences Naturelles, 118*(9), 1–14.

Sommaruga, A. (1999). Décollement tectonics in the Jura foreland fold-and-thrust belt. *Marine and Petroleum Geology, 16,* 11–134.

Sommaruga, A., Eichenberger, U., & Marillier, F. (2012). Seismic Atlas of the Swiss Molasse Basin. Edited by the Swiss Geophysical Commission. - Matér. Géol. Suisse, Géophys. 44.

Thouvenot, F., Frechet, J., Tapponnier, P., Thomas, J., Le Brun, B., Menard, G., et al. (1998). The ML 5.3 Epagny (French Alps) earthquake of 1996 July 15: A long-awaited event on the Vuache Fault. *Geophysical Journal International, 135,* 876–892.

Townend, J., & Zoback, M. D. (2000). How faulting keeps the crust strong. *Geology, 28*(5), 399–402.

von Hagke, C., Cederbom, C. E., Oncken, O., Stöckli, D. F., Rahn, M. K., & Schlunegger, F. (2012). Linking the northern Alps with their foreland: The latest exhumation history resolved by low-temperature thermochronology. *Tectonics, 31*(5), TC5010. doi:10.1029/2011TC003078.

von Hagke, C., Oncken, O., & Evseev, S. (2014). Critical taper analysis reveals lithological control of variations in detachment strength: An analysis of the Alpine basal detachment (Swiss Alps). *Geochemistry, Geophysics, Geosystems, 15*(1), 176–191. doi:10.1002/2013GC005018.

Vouillamoz, N. (2015). *Microseismic characterization of Fribourg area (Switzerland) by Nanoseismic Monitoring*. Ph.D. dissertation, GeoFocus 38, University of Fribourg, Fribourg, Switzerland, 278 pp.

Vouillamoz, N., Wust-Bloch, G. H., Abednego, M., & Mosar, J. (2016). Optimizing event detection and location in low-seismicity zones: Case study from western Switzerland. *Bulletin of the Seismological Society of America, 106*(5), 2023–2036. doi:10.1785/0120160029.

Wiemer, S., Giardini, D., Fäh, D., Deichmann, N., & Sellami, S. (2009). Probabilistic seismic hazard assessment of Switzerland: Best estimates and uncertainties. *Journal of Seismology, 13*(4), 449–478. doi:10.1007/s10950-008-9138-7.

Willett, S. D., & Schlunegger, F. (2010). The last phase of deposition in the Swiss Molasse basin: From foredeep to negative-alpha basin. *Basin Research, 22*(5), 623–639. doi:10.1111/j.1365-2117.2009.00435.x.

Wust-Bloch, G. H., & Joswig, M. (2006). Pre-collapse identification of sinkholes in unconsolidated media at Dead Sea area by 'nanoseismic monitoring' (graphical jackknife location of weak sources by few, low-SNR records). *Geophysical Journal International, 167*(3), 1220–1232. doi:10.1111/j.1365-246X.2006.03083.x.

Zoback, M. D. (2007). *Reservoir geomechanics*. Cambridge: Cambridge University Press.